SPANDIDOS PUBLICATIONS

INTERNATIONAL JOURNAL OF ONCOLOGY 54: 1099-1111, 2019

Lidocaine induces protective autophagy in rat C6 glioma cell line

MAGDALENA IZDEBSKA[1], MARTA HAŁAS-WIŚNIEWSKA[1], WIOLETTA ZIELIŃSKA[1], ANNA KLIMASZEWSKA-WIŚNIEWSKA[2], DARIUSZ GRZANKA[2] and MACIEJ GAGAT[1]

Departments of [1]Histology and Embryology, and [2]Clinical Pathomorphology, Faculty of Medicine, Nicolaus Copernicus University in Toruń, Collegium Medicum in Bydgoszcz, 85-092 Bydgoszcz, Poland

Received August 14, 2018; Accepted November 16, 2018

DOI: 10.3892/ijo.2018.4668

Abstract. Malignant glioma is the most common type of brain cancer with poor prognosis. Surgical resection, chemotherapy and radiotherapy are the main therapeutic options; however, in addition to their insufficient efficacy, they are associated with the pain experienced by patients. To relieve pain, local anesthetics, such as lidocaine can be used. In the present study, the effects of lidocaine on the C6 rat glioma cell line were investigated. An MTT assay and Annexin V/propidium iodide analysis indicated the increase in the percentage of apoptotic and necrotic cells in response to lidocaine. Furthermore, light microscopy analysis on the ultrastructural level presented the occurrence of vacuole-like structures associated with autophagy, which was supported by the analysis of autophagy markers (microtubule-associated protein 1A/1B-light chain 3, acridine orange and Beclin-1). Additionally, reorganization of the cytoskeleton was observed following treatment with lidocaine, which serves an important role in the course of autophagy. To determine the nature of autophagy, an inhibitor, bafilomycin A1 was applied. This compound suppressed the fusion of autophagosomes with lysosomes and increased the percentage of apoptotic cells. These results demonstrated that lidocaine may induce cytoprotective autophagy and that manipulation of this process could be an alternative therapeutic strategy in the treatment of cancer.

Introduction

Gliomas pose as a serious issue in the field of neurooncology as they represent ~30% of all brain tumors and 80% of all malignant brain tumors (1). Furthermore, gliomas tend to be incurable and the median survival is dependent on the tumor type. Patients diagnosed with low-grade tumors exhibit a median survival of >10 years (2). The outcome is notably different in the case of high-grade gliomas, for which the median survival varies between 3 years for anaplastic glioma and 15 months for glioblastoma multiforme (3). In addition, there are few therapeutic solutions for the treatment of gliomas. One of the most favorable approach is the combination of chemo- and radiotherapy with surgical intervention (4); however, none of the currently available methods provide satisfying results. Additionally, as described by Neeman and Ben-Eliyahu (5), surgery does not only enhance the passage of malignant cells into the blood and lymphatic vessels, but also inhibits the apoptosis of abnormal cells and increases their invasiveness, which correlates with higher metastatic ability. Furthermore, alterations in the immune and neuroendocrine systems in the response to surgery have been associated with the promotion of cancer progression (6).

For patients, one of the most notable symptom associated with surgical glioma excision is pain. As a preventative measure, local anesthetics, such as lidocaine can be used. In addition to analgesia, these agents may possess other beneficial properties. Lidocaine exhibits its activity by blocking voltage-gated sodium channels (VGSC) on nociceptors, which leads to the elimination of pain; however, these receptors are expressed on the surface of some cancer cells (7-9). In the case of cancer, increased expression of VGSC has been demonstrated in some highly metastatic lines compared with low-metastatic lines (10). In addition, the blockage of these channels by chemical agents leads to reduced invasiveness (11,12). This indicates the importance of VGSC in the metastatic process. Therefore, the effects of lidocaine on cancer cells requires further investigation. As reported by numerous studies, lidocaine and other local anesthetic drugs decrease the growth, invasiveness and migration potential of non-small-cell lung carcinoma, breast cancer or human hepatocellular carcinoma cells (13-16). Recently, the anti-proliferative effects of lidocaine on glioma cells was reported (17); however, in this case lidocaine activity may be associated with the inhibition of the melastatin-like transient receptor potential 7 (TRPM7) action.

Local anesthetics have been proposed to induce the death of cancer cells via the apoptotic and necrotic pathways (18-20); however, our current research also indicates the occurrence of autophagy. In normal cells, autophagy aims to degrade unnecessary or damaged organelles, and proteins (21). In cancer cells, this process serves different roles. In the early stages of cancer, when the tumor is not yet vascularized, autophagy can serve the cell as a way to obtain nutrition;

Correspondence to: Dr Maciej Gagat, Department of Histology and Embryology, Nicolaus Copernicus University in Toruń, Collegium Medicum in Bydgoszcz, 24 Karłowicza Street, Bydgoszcz 85-092, Poland
E-mail: mgagat@cm.umk.pl

Key words: glioma cell line, autophagy, apoptosis, lidocaine

thus, tumorigenesis is induced. Conversely, mutations in the genes responsible for autophagy are generally associated with enhanced progression of cancer (22-24). There are two explanations for this. The first is that autophagy inhibition leads to increased necrosis rate, which is associated with the inflammatory response and thus cancer development. The second may be rapid accumulation of mutations due to the lack of counteracting the effects of increased oxidative stress by autophagy (25); however, in all cases, autophagy is be easily detected by observing characteristic structures, including the autophagosome and autophagolysosomes (26).

The present study aimed to determine the effects of lidocaine on rat C6 glioma cells; this local anesthetic induces protective autophagy. From a clinical point of view, the findings of the present study suggests that the use of lidocaine in a patient with glioma should be carefully considered. We also propose to use other anesthetic agents preferentially.

Materials and methods

Cell culture and treatment. C6, a rat glioma cell line, was purchased from American Type Culture Collection (CCL-107, Manassas, VA, USA). The cells were cultured in tissue culture flasks or 12-well plates (BD Biosciences, Franklin Lakes, NJ, USA) and grown as a monolayer at 37˚C in a humidified CO_2 incubator (5% CO_2) in Ham's F12 medium (Lonza Group, Ltd., Basel, Switzerland). The medium was supplemented with 10% fetal bovine serum, 2 mM glutamine and 50 μg/ml gentamycin (both from Sigma-Aldrich; Merck KGaA, Darmastadt, Germany). C6 cells were treated for 24 h in 37˚C (incubator) with 0.25, 0.5, 1, 5, 10, 15 and 30 mM of lidocaine (Sigma-Aldrich; Merck KGaA) for the MTT assay and 5, 10 and 15 mM for other experiments. The control cells were grown under the same conditions in the absence of lidocaine. In order to inhibit autophagy, the cells were pretreated with 100 nM bafilomycin A1 (Baf A1; Sigma-Aldrich; Merck KGaA) for 4 h in 37˚C and then incubated in the presence or absence of lidocaine for 24 h in 37˚C The C6 culture was tested for *Mycoplasma* based on the rapid staining with DAPI (Sigma-Aldrich; Merck KGaA). The staining process was conducted for 10 min at room temperature. The tests were negative. All *in vitro* studies were performed on ells of low passage number (<5). Following 24 h of incubation with lidocaine (37˚C), the cells were observed using an inverted microscope (magnification, x40; Nikon Corporation, Tokyo, Japan), at least 5 number of fields per view, which provided the basis for further analysis.

MTT assay. The cytotoxic effect of lidocaine on cell viability was assessed using a colorimetric MTT metabolic activity assay. The cells were cultured in 12-well plates ($0.11x10^6$) for 24 h and then treated with 0.25, 0.5, 1, 5, 10, 15 and 30 mM of local anesthetic for another 24 h (37˚C). The MTT stock solution was prepared by dissolving MTT (Sigma-Aldrich; Merck KGaA) in 5 mg/ml PBS. Following lidocaine treatment, the cells were washed with PBS and incubated with MTT solution which was mixed with Dulbecco's modified Eagle's medium without phenol red (Lonza Group, Ltd. in the ratio 1:9 for 3 h at 37˚C. MTT was reduced by metabolically active cells to insoluble purple formazan crystals which were dissolved in isopropanol (2 ml); cells were centrifuged at 15,717 x g for 2 min at room temperature. The absorbance was measured at the wavelength of 570 nm using a spectrophotometer (Spectra Academy, K-MAC, Daejeon, Korea). The viability of glioma cells was expressed as the percentage relative to the control cells, which was assumed as 100%. The viability of cells pretreated with Baf A1 also was studied using an MTT assay. The experiment was conducted in the same manner as for cells without Baf A1 pretreatment. After analyzing the results 5, 10 and 15 mM lidocaine concentrations were used for subsequent experiments.

Cell death analysis. The apoptosis kssay kit containing propidium iodide (PI), Annexin V Alexa Fluor® 488 and Propidium Iodide (Invitrogen; Thermo Fisher Scientific, Inc., Waltham, MA, USA) was used to measure the percentage of viable, apoptotic and necrotic cells by detecting phosphatidyl serine expression and membrane permeability. On this basis the populations of cells were detected as Annexin V-negative/PI-negative (live), Annexin V-positive/PI-negative (early apoptosis), Annexin V-positive/PI-positive (late apoptosis) or Annexin V-negative/PI-positive (necrosis). The procedure was performed according to the manufacturer's protocols. After 24 h incubation (37˚C) of C6 cells with lidocaine (5, 10 and 15 mM), the cells were trypsinized (0.25% trypsin solution, 37˚C, 5 min), centrifuged (500 x g, 8 min, room temperature) and suspended in Annexin binding buffer included in the applied kit (ABB, 100 μl). Subsequently, to each 100 μl of sample, 5 μl Annexin V Alexa Fluor 488 was added and incubated in dark for 20 min at room temperature. After this time, the cells were centrifuged (300 x g, 5 min at room temperature, resuspended in 100 μl ABB again and 1 μl PI was added for 3 min to each sample at room temperature. The data were analyzed using a Guava easyCyte 6HT-2L Benchtop Flow Cytometer (Merck KGaA) and FlowJo vX0.7 software (FlowJo LLC, Ashand, OR, USA). The cells pretreated with Baf A1 were also assessed using the Annexin V Alexa Fluor® 488 and Propidium Iodide assay and the experiment was conducted in the same manner as for cells without Baf A1 pretreatment.

Cell cycle analysis. Alterations in the cell cycle of C6 cells after 24 h treatment with lidocaine (5, 10 and 15 mM) were investigated using Tali Cell Cycle Kit (Invitrogen; Thermo Fisher Scientific, Inc.) according to the manufacturer's protocols. Briefly, the treated cells ($0.11x10^6$) were trypsinzed (0.25% trypsin solution, 37˚C, 5 min), centrifuged (500 x g, 8 min at room temperature) and fixed in ice-cold 70% ethanol (-18˚C, 24 h). The next day, after washing with PBS and centrifugation (500 x g, 7 min at room temperature), the cells were resuspended in the Tali Cell Cycle Solution. After 30 min of incubation at room temperature, the data were determined using Guava easyCyte 6HT-2L Benchtop Flow Cytometer. The percentage of cells in each phase of the cell cycle was assessed using FlowJo vX0.7 software.

Morphological and ultrastructural analysis

Light microscopy. For the morphological analysis of the C6 cells following treatement with lidocaine the cells were seeded onto 12-well plate in density of $0.11x10^6$. After 24 h the cells

were treated with appropriate doses of lidocaine (5, 10 and 15 mM at 37˚C) or left untreated in the case of control group. After another 24 h, hematoxylin staining was conducted. First, the cells were fixed with 4% paraformaldehyde (pH 7.4; PA, SERVA Electrophoresis GmbH, Heidelberg, Germany), rinsed three times with PBS and washed with dH_2O. For nuclear staining, Mayer's hematoxylin was used (3 min at room temperature). Subsequently, the cells were rinsed under tap water and washed with PBS. The preparations were mounted using Aqua PolyMount (Polysciences, Inc., Warrington, PA, USA). The morphology of cell was observed using an Eclipse E800 light microscope (Nikon Corporation; x40 magnification with at least 10-20 fields per view analyzed) and NIS-Elements 4.0 software (Nikon Corproation).

Transmission electron microscopy (TEM). As an indicator of autophagy, vacuoles were detected by TEM. For this reason the cells were seeded onto 6-well plate in density of 0.4x106. After 24 h incubation with lidocaine, the C6 cells were fixed for 30 min with 3.6% (v/v) glutaraldehyde (6˚C; Polysciences, Inc.) in 0.1 M sodium cacodylate buffer (pH 7.4; Carl Roth GmbH + Co. KG, Karlsruhe, Germany) and washed with 0.1 M sodium cacodylate buffer. The cells were then entrapped within fibrin clots at room temperature, which consist of bovine thrombin (50 U/ml) (Biomed-Lublin, Lublin, Poland) and fibrinogen (3 mg/ml; Sigma-Aldrich; Merck KGaA). Then, the cells were post-fixed with 1% (w/v) osmium tetroxide (SERVA Electrophoresis GmbH) in 0.1 M sodium cacodylate buffer for 1 h at room temperature. The samples were rinsed with sodium cacodylate buffer and dehydrated via a graded ethanol (30-90%) and acetone (90-100%) (both from Avantor Performance Materials Poland S.A., Gliwice, Poland) series. The studied material was then embedded in epoxy resin (Epon 812; Carl Roth GmbH + Co. KG), in which polymerization was carried out at 37˚C for 24 h and then at 65˚C for 5 days. Following polymerization, the selected part of material was cut into ultrathin sections (65 nm) using a Reichert Om-U3 ultramicrotome (Leica Microsystems, Inc., Buffalo Grove, IL, USA), placed on copper grids and counterstained with 1% uranyl acetate (7 min at room temperature; Ted Pella, Inc., Redding, CA, USA). The samples were examined using a TEM JEM 100 CX (JEOL, Ltd., Tokyo, Japan); at least 15-20 fields per view were analyzed.

Fluorescent staining

Acridine orange (AO) staining. To detect the typical structures for autophagy, such as acidic vesicular organelles (AVOs), AO (Sigma-Aldrich; Merck KGaA) was used. The C6 glioma cells were seeded on coverslips in 12-well plates ($0.11x10^6$ of cells) and treated with lidocaine for 24 h. Subsequently, the cells were incubated in medium containing 1 μg/ml AO for 15 min at 37˚C. Then, the medium was removed, the cells were rinsed with PBS at room temperature and immediately examined with Nikon Eclipse E800 fluorescence microscope and NIS-Elements 4.0 software (Nikon Corporation). Additionally, AVOs were studied using a Guava easyCyte 6HT-2L Benchtop Flow Cytometer. Flow cytometry data were analyzed using FlowJo vX0.7 software.

Immunofluorescence staining of LC3-II. To detect microtubule-associated protein 1A/1B-light chain 3 (LC3)-II protein, the cells were seeded on coverslips ($0.11x10^6$ cells) and treated with lidocaine in the concentrations of 5, 10 and 15 mM (37˚C). After 24 h incubation with lidocaine the cells were fixed with 4% paraformaldehyde for 20 min at room temperature, rinsed with PBS and permeabilized with 0.25% Triton X-100 (SERVA Electrophoresis GmbH). Then, to block nonspecific binding sites, 1% (w/v) bovine serum albumin (BSA; Sigma-Aldrich; Merck KGaA) in PBS was used (20 min at room temperature). Then, the cells were incubated with rabbit anti-LC3-II antibody (1:2,000; Thermo Fisher Scientific, Inc., cat. no. PA1-46286) for 1 h at room temperature, and Alexa Fluor 488-labeled goat anti-rabbit secondary antibody (1:100; Invitrogen; Thermo Fisher Scientific, Inc., cat. no. A27034) for 1 h at room temperature. Following washing with PBS, the cell nuclei were stained with DAPI (1:20,000; Sigma-Aldrich; Merck KGaA) for 10 min at room temperature. Finally, the slides were mounted with Aqua-Poly/Mount and examined using a Nikon Eclipse E800 fluorescence microscope (magnification, x40 in at least 10-20 fields per view) and NIS-Elements 4.0 software.

Fluorescence staining of cytoskeletal proteins (tubulin, vimentin and actin). The C6 cells following treatment with lidocaine were cultured on glass coverslips (24 h, 37˚C). For β-tubulin staining, the cells were prefixed with bifunctional protein crosslinking reagent dithiobis(succinimidyl propionate) (DTSP; 1 mM 3,30-dithiodipropionic acid) diluted 1:50 in Hanks' Balanced Salt solution (both from Sigma-Aldrich; Merck KGaA) for 10 min (RT). Then, the cells were permeabilized in TSB (0.5% Triton X-100) SERVA Electrophoresis GmbH] in microtubule stabilizing buffer (MTSB; 1 mM EGTA, 10 mM PIPES, 4% poly(ethylene glycol); Sigma-Aldrich; Merck KGaA) with the addition of DTSP (in dimethyl sulfoxide) for 10 min and rinsed with TSB for 5 min. The cells were fixed with 4% paraformaldehyde in MTSB for 15 min (room temperature), washed with PBS and incubated with 1% BSA diluted in Tris-buffered saline for 15 min (room temperature). Tubulin was labeled using a mouse monoclonal antibody against β-tubulin (Sigma-Aldrich; Merck KGaA, cat. no. T5293) and anti-rabbit antibody-Alexa Fluor 488 (Invitrogen; Thermo Fisher Scientific, Inc., cat. no. A27034).

In the case of F-actin and vimentin labeling, the cells were fixed with 4% paraformaldehyde in PBS, for 15 min, treated with 0.25% Triton X-100 for 5 min and blocked in 1% (w/v) BSA/**PBS at room temperature. To stain F-actin, phal**loidin-tetramethylrhodamine (Sigma-Aldrich; Merck KGaA, cat. no. P1951) was used and vimentin was detected by using mouse anti-vimentin antibody (Sigma-Aldrich; Merck KGaA, cat. no. V6630) and anti-mouse antibody-Alexa Fluor 488 (Invitrogen; Thermo Fisher Scientific, Inc., cat. no. A27034). As aforementioned, cell nuclei were stained with DAPI and the slides were mounted in Aqua-Poly/Mount. All slides were examined using a Nikon Eclipse E800 fluorescence microscope (magnification, x40, in at least 10-20 fields per view) and NIS-Elements 4.0 software.

Reverse transcription-quantitative polymerase chain reaction (RT-qPCR) analysis. Total RNA from C6 cells was extracted using the Total RNA Mini Plus kit (A&A Biotechnology, Gdynia, Poland) according to the manufacturer's protocols,

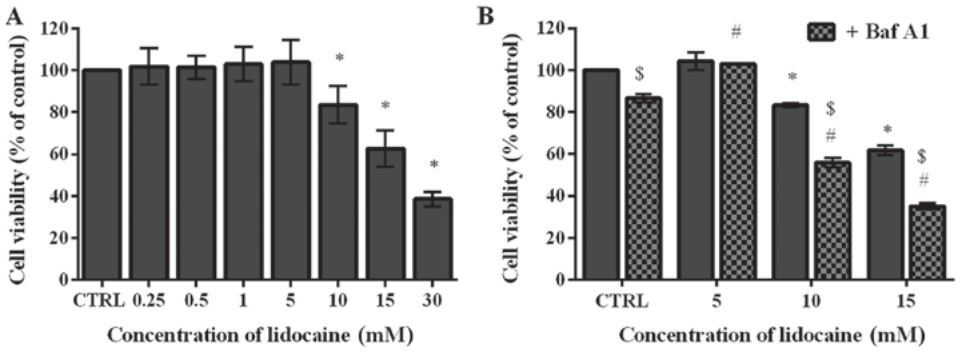

Figure 1. Effect of lidocaine on the rat C6 glioma cells. Cell viability was determined by MTT colorimetric assay. Data are presented as a percentage of the control. (A) Cells treated with various concentrations of lidocaine (0.25, 0.5, 1, 5, 10, 15 and 30 mM) for 24 h. Control cells were cultured under identical conditions, but without lidocaine. *P<0.05 lidocaine doses vs. CTRL. (B) Viability of cells pretreated with Baf A1 (inhibitor of autophagy) and treated with 5, 10 and 15 mM lidocaine. #P<0.05 lidocaine doses + Baf A1 vs. CTRL + Baf A1. $P<0.05 cells pretreated with Baf A1 and then treated with lidocaine vs. cells treated just with lidocaine. Baf A1, bafilomycin A1; CTRL, control.

followed by the spectrophotometric determination of the concentration and purity of the obtained RNA (BioSpectrometer basic; Eppendorf, Hamburg, Germany). A one-step RT-qPCR was performed with LightCycler RNA Master SYBR Green I kit (Roche Applied Science, Mannheim, Germany) on a LightCycler 2.0 Instrument (Roche Applied Science). The total reaction mixture (20 μl per single LightCycler capillary) contained 100 ng of RNA and 0.2 μM of each primer in addition to the LightCycler RNA Master SYBR-Green I kit components. The sequences of primers were as follows: Beclin-1 (*Becn1*, forward, 5'-AGCTGCCGTTATACTGTT CTG-3' and reverse, 5'-ACTGCCTCCTGTGTCTTCAAT CTT-3'; *LC3B*, forward, 5'-GCCTTCTTCCTCCTGGTGAAT-3' and reverse, 5'-TTTTTGCCTTGGTAGGGGCTT-3'; and *GAPDH*, forward, 5'-CACTGAGCATCTCCCTCACAA-3' and reverse, 5'-TGGTATTCGAGAGAAGGGAGG-3'. The thermocycling conditions were as follows: RT for 20 min at 61˚C (one cycle); qPCR was conducted with denaturation for 1 min at 95˚C (one cycle) and 45 cycles of denaturation for 5 sec at 95˚C, followed by annealing and extension for 20 sec at 57-61˚C (depending on the melting temperature of the primers) and 5 sec at 72˚C, respectively. The data obtained from at least three independent experiments were analyzed with LightCycler Software Version 4.0 (Roche Applied Science). The relative gene expression was normalized to that of GAPDH internal control and assessed using the $2^{-\Delta\Delta Cq}$ method (27).

Statistical analysis. The data were presented as the mean ± standard deviation. GraphPad Prism 6.0 software (GraphPad Software, Inc., La Jolla, CA, USA) was used for statistical analyses. A one sample t-test was performed to analyze MTT and RT-qPCR data as it compares the mean with a hypothetical value (100 or 1). A nonparametric Kruskal-Wallis test with Dunn's post hoc test or the one-way analysis of variance with Tukey's post hoc test (ANOVA, normal distributions) were used to evaluate the differences in mean values between cells treated with lidocaine compared with the control (cells with and without Baf A1 pretreatment), independently (cell death and RT-qPCR). In the case of multiple comparison the two-way ANOVA was performed with Dunnett's multiple comparisons test (cell cycle, fluorescence intensity of AO). P<0.05 was considered to indicate a statistically significant difference.

Results

Lidocaine decreases the viability of glioma C6 cells. To determine the cytotoxic effect of lidocaine on the rat glioma cells, an MTT assay was conducted. During surgical interventions, 5-20 mM lidocaine is applied (28); thus for the first step of the investigation 0.25, 0.5, 1, 5, 10, 15 and 30 mM were selected in the present study. The lowest four concentrations exhibited limited impact on the C6 cells. The cell viability following treatment with these low doses slightly increased by 1.72, 1.43, 2.97 and 3.95%, respectively, compared with the control, which was assumed as 100%. Conversely, treatment with higher doses (10, 15 and 30 mM) resulted in 83.48, 62.63 and 38.59% cell viability, respectively, which was significantly lower compared with the control (Fig. 1A). The MTT assay was also applied to assess the viability of cells pretreated with Baf A1, which inhibits autophagy by preventing the fusion of autophagosomes and lysosomes (29). In cells incubated with Baf A1 for 4 h, the viability significantly decreased to 86.54% compared with the untreated cells. Following treatment with the lowest dose of lidocaine (5 mM), significant differences between untreated cells and those pretreated with Baf A1 were not observed; however, pretreatment with the inhibitor of autophagy followed by incubation with 10 and 15 mM lidocaine induced significant decreases in cell viability compared with cells treated with lidocaine alone; the percentage of live cells amounted to 55.91 and 35.18%, respectively (Fig. 1B). Additionally, we observed statistically significant differences between cells treated with lidocaine and Baf A1, and the control (Fig. 1B).

Lidocaine induces cell death mainly by necrosis. To assess the mechanism underlying the cytotoxic effect of lidocaine on the glioma cell line, Annexin V and PI staining was applied. The percentage of live, apoptotic and necrotic cells was analyzed in the populations treated only with lidocaine and pretreated with Baf A1. Following treatment with lidocaine alone, a dose-dependent decrease in the live cell population was observed. In the control, the percentage of live cells amounted to 93.26%, which significantly decreased to 81.16, 78.57 and 59.98% after treatment with 5, 10 and 15 mM lidocaine, respectively (Fig. 2A). The number of live cells were significantly lower when Baf A1 was applied. Following

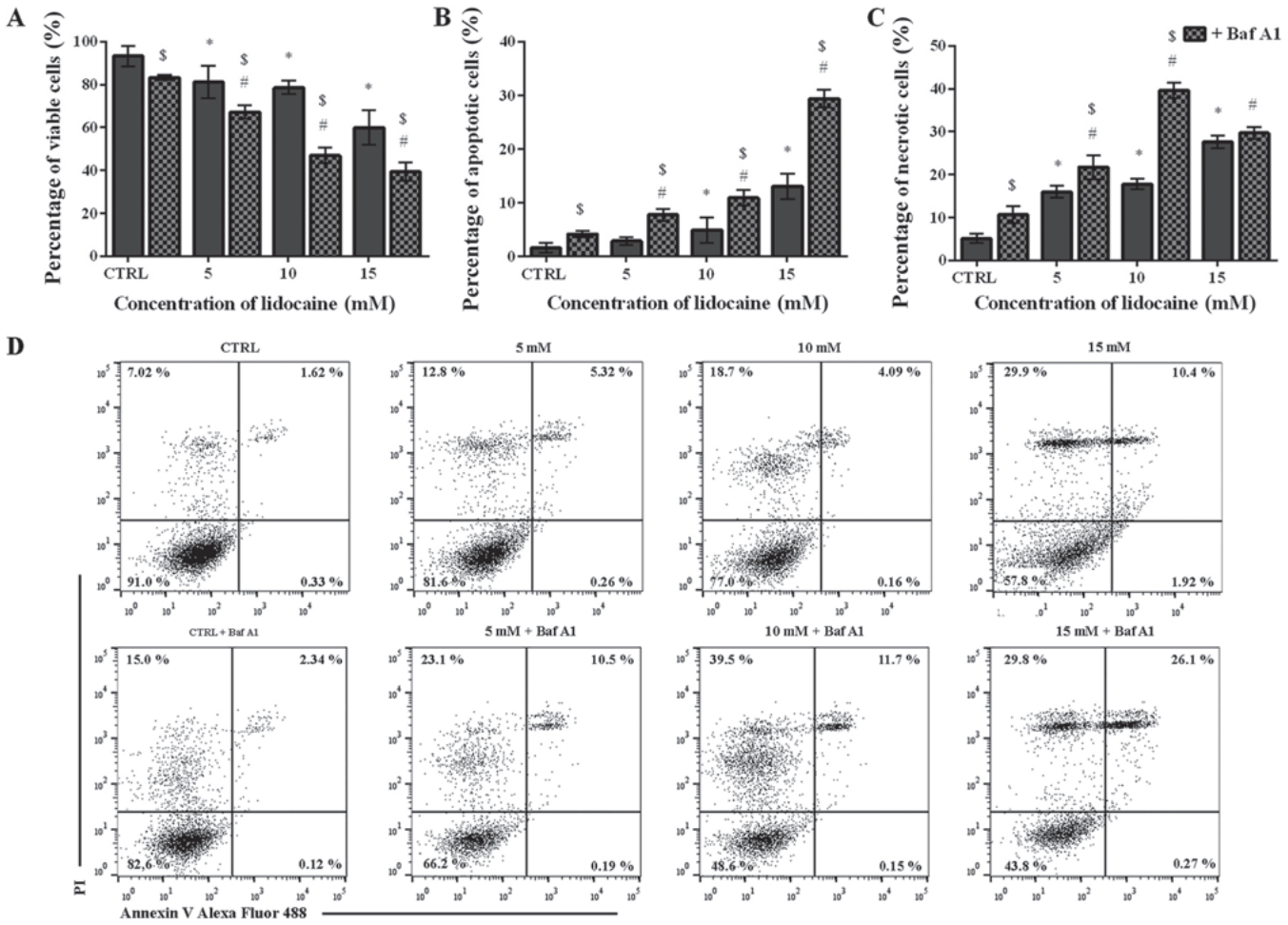

Figure 2. Effect of lidocaine on the induction of cell death. Annexin V/PI assay was carried out by flow cytometry. Cells were treated with various concentrations of lidocaine (5, 10 and 15 mM) for 24 h, and with or without Baf A1 pretreatment. (A) Percentage of live cells (Annexin V and PI-negative); (B) percentage of apoptotic cells. The sum of the early and late apoptotic cells represented the total apoptosis [Annexin V-positive/PI-negative (early apoptosis or Annexin V/PI-positive (late apoptosis)]; (C) percentage of necrotic cells (Annexin V-negative/PI-positive). (D) Representative plots for the cell death analysis. *P<0.05, lidocaine doses vs. CTRL. #P<0.05 lidocaine doses + Baf A1 vs. CTRL + Baf A1. $P<0.05 cells pretreated with Baf A1 and then treated with lidocaine vs. cells treated with lidocaine. Baf A1, bafilomycin A1; CTRL, control; PI, propidium iodide.

pretreatment with the inhibitor of autophagy, 83.27% of live cells was noted; however, when 5, 10 and 15 mM lidocaine were added, the percentage of live cells was significantly lower compared with lidocaine treatment alone and reached 67.24, 46.94 and 39.47%, respectively (Fig. 2A). In C6 cells treated with 5, 10 and 15 mM lidocaine, the percentage of apoptotic cells increased from 1.58% in the control to 2.88, 4.93 and 13.06%, respectively; however, only in the case of 10 and 15 mM lidocaine, the differences were statistically significant. Furthermore, the percentage of apoptotic cells was increased in response to pretreatment with Baf A1. In control cells treated only with inhibitor of autophagy, the percentage of apoptotic cells amounted to 4.19%; following incubation with 5, 10 and 15 mM lidocaine the number of apoptotic cells significantly increased to 7.78, 10.93 and 29.38%, respectively (Fig. 2B).

As presented in Fig. 2C, the population of necrotic cells increased in a dose-dependent manner from 5.11% to 15.95, 17.77 and 27.62% after treatment with 5, 10 and 15 mM lidocaine, respectively. In the case of cells pretreated with Baf A1 alone, the number of necrotic cells was significantly higher compared with the untreated control and amounted to 10.66%; the number of necrotic cells significantly increased to 21.74, 39.62 and 29.69% following Baf A1 pretreatment and incubation with increasing lidocaine concentrations. However, significant differences were not observed following treatment with 15 mM lidocaine in the presence or absence of Baf A1 (Fig. 2C). Representative plots are presented in Fig. 2D.

Lidocaine treatment induces alters the cell cycle distribution. The cell cycle was analyzed using flow cytometry. A significant increase from 58.15% in the control to 65.87 and 66.72% in the percentage of cells with DNA content corresponding to G0/G1 phase was observed following treatment with 5 and 10 mM lidocaine, respectively (Fig. 3). The results obtained for the control cells were similar to that after treatment with lidocaine (15 mM). The population of cells in S-phase reached 8.35, 8.02, 7.44 and 8.71% in the control and cells treated with 5, 10 and 15 mM lidocaine, respectively; however, the results were not statistically significant (Fig. 3). Following incubation with 5 and 10 mM lidocaine, a significant decrease in the number of cells in G2/M phase compared with the control was noted (Fig. 3). In the control, the mean percentage of cells with DNA content corresponding to G2/M phase amounted to 29.75%, and following treatment with 5 and 10 mM lidocaine decreased

to 22.20 and 22.40%, respectively. In turn, after incubation with the highest dose of lidocaine, the population of cells in G2/M phase of cell cycle was similar to the control cells. In addition, a slight difference in the percentage of polyploid cells (2.78% in the control cells, and 3.66, 2.37 and 2.92% following treatment with 5, 10 and 15 mM lidocaine, respectively) (Fig. 3).

Lidocaine induces the formation of autophagic vacuoles. Small vacuole-like structures were observed under an inverted microscope following treatment with lidocaine. A spindle-shaped morphology, which is typical for C6 cells, was visible in the control and treatment with the lowest dose of lidocaine, whereas following incubation with 10 and 15 mM of lidocaine, numerous vacuoles in the cytoplasm of C6 cells had formed (Fig. 4). The same results were observed after hematoxylin staining. TEM was used to assess cell morphology on the ultrastructural level. As presented in Fig. 4, cells incubated with lidocaine in 10 and 15 mM exhibited numerous vacuole-like structures in the cytoplasm area compared with the control cells. Furthermore, following treatment with the lowest dose of lidocaine, fewer, small vacuoles, which were not visible via light microscopy, were also observed by TEM. Some of these structures contained amorphous materials and organelles in the various stages of degeneration. Higher doses of lidocaine revealed larger vacuoles. Additionally, the majority of them were enclosed by a single membrane, which suggests autolysosome formation. The ultrastructural feature of autophagy, swollen mitochondria with disorganized cristae was also observed (Fig. 4).

Lidocaine induces autophagy. LC3 is a specific marker of autophagy and exists in varied forms. LC3-I (18 kDa) is present in the cytosol, and undergoes proteolysis and lipid modification for conversion into LC3-II (16 kDa) (30). The shorter form is located in the membrane of autophagosomes whereby the expression levels of LC3-II correspond to the amount of these structures (31). In control cells and after treatment with the lowest dose of lidocaine, the fluorescence staining of LC3-II was poor and diffuse , but following treatment with higher doses of lidocaine the punctate pattern of LC3-II expression was observed. Based on the images from fluorescence microscopy, increased LC3-II staining occurred in response to 10 mM lidocaine than with the highest dose (Fig. 5A). The punctate accumulation of LC3-II following pretreatment of cells with Baf A1 and incubation with 10 mM lidocaine was also noted, which is consistent with the inhibition of autophagy (Fig. 5B).

In addition, lidocaine treatment led to a significant dose-dependent increase in the transcript expression level of *LC3B* compared with the control (Fig. 6A). To further investigate the occurrence of autophagy, the mRNA expression levels of another autophagy marker, *Becn1*, were examined following treatment with lidocaine. As presented in Fig. 6B, this agent significantly upregulated the mRNA expression of *Becn1*; the expression levels were notably lower in response to 10 mM lidocaine compared with the other treatment groups.

The second fluorescence method was staining with AO. AO labels AVOs, such as autolysosomes and is also used in autophagy assays. In AO-stained cells, the cytoplasm and nucleus fluoresced bright green, whereas AVOs fluoresced bright red. The intensity of red fluorescence is proportional to the degree of acidity and the acidic compartment volume (32). In

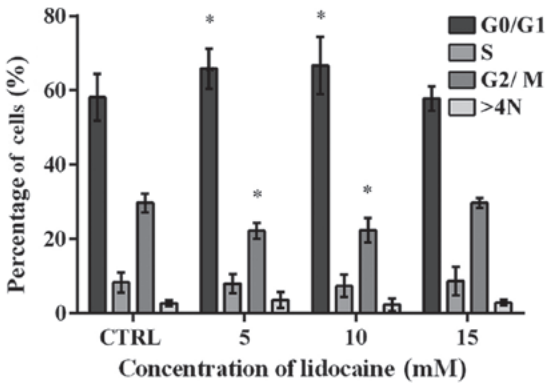

Figure 3. Alterations in the cell cycle distribution following treatment with lidocaine as determined by flow cytometry. Cells were treated with various concentrations of lidocaine (5, 10 and 15 mM) for 24 h. The percentage of cells in G0/G1 phase, S phase and G2/M, phase and with >4N DNA content. *P<0.05 lidocaine doses vs. CTRL. CTRL, control.

control C6 glioma cells and cells treated with 5 mM lidocaine, few AVOs (punctate fluorescence) were observed. Lidocaine (10 and 15 mM) promoted the formation of AVOs; however, more were detected following treatment with 10 mM lidocaine compared with the highest dose (Fig. 7A). Additionally, in the cells pretreated with Baf A1 and incubated with 10 mM lidocaine, the signal of red fluorescence was almost completely blocked (Fig. 7B). The results were confirmed by using flow cytometry. In addition, the mean fluorescence intensity of AO was the highest in C6 cells treated with 10 mM lidocaine; a significant increase in the mean fluorescence intensity was also observed following treatment with 15 mM lidocaine compared with the control. Pretreatment with Baf A1 revealed significant decreases in the mean fluorescence intensity compared with the untreated control (Fig. 7C).

Lidocaine induces alterations in the organization of the main cytoskeletal components. The cytoskeleton is a very important organelle in the cell which undergoes reorganization during numerous cellular processes (33,34). The results of the present study revealed that lidocaine induced notable alterations in the organization of cytoskeleton of glioma cells, which was associated with autophagic structure formation. Control cells were characterized by highly-developed F-actin with long stress fibers in the cytoplasm, cytoplasmic protrusions and regions of cell-cell junctions (Fig. 8). Following treatment with the lowest dose of lidocaine, marked changes in microfilament structure were not observed (Fig. 8). Treatment with 10 and 15 mM lidocaine demonstrated the reorganization of actin filaments (Fig. 8). These cells exhibited a diffuse network of F-actin with short actin fibers and/or small, punctate accumulation within the cytoplasm. The accumulation of actin in the cortical region of cells following incubation with 10 mM lidocaine was also observed (Fig. 8). In small, shrunken cells the intensity of actin fluorescence increased.

The fluorescence staining of β-tubulin also presented marked lidocaine-induced alterations in the organization of microtubules and mitotic spindle morphology (Fig. 8). In the control cells and cells incubated with the lowest dose of lidocaine, β-tubulin was organized in a regular and dense network of long microtubules, which radiated from the

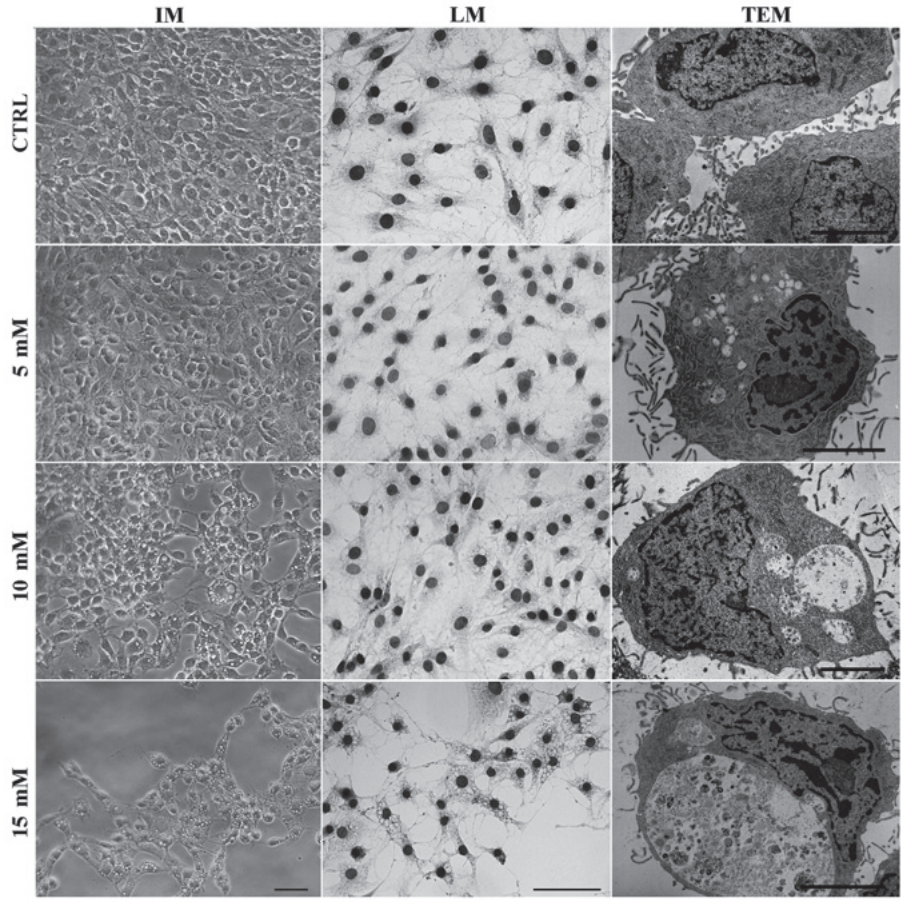

Figure 4. Lidocaine induces autophagic vacuole formation in rat glioma cell line. The effects of lidocaine were evaluated by IM in C6 cells following treatment with various concentrations of lidocaine (5, 10 and 15 mM) for 24 h. Scale bar, 50 μm. Hematoxylin staining (LM) of CTRL cells, and cells treated with 5, 10 and 15 mM lidocaine. Scale bar, 50 μm. The detection of autophagic-like vacuoles using TEM in control cells and incubated with 5, 10 and 15 mM lidocaine. Scale bar, 10 μm. CTRL, control; IM, inverted microscopy; LM, light microscopy; TEM, transmission electron microscopy.

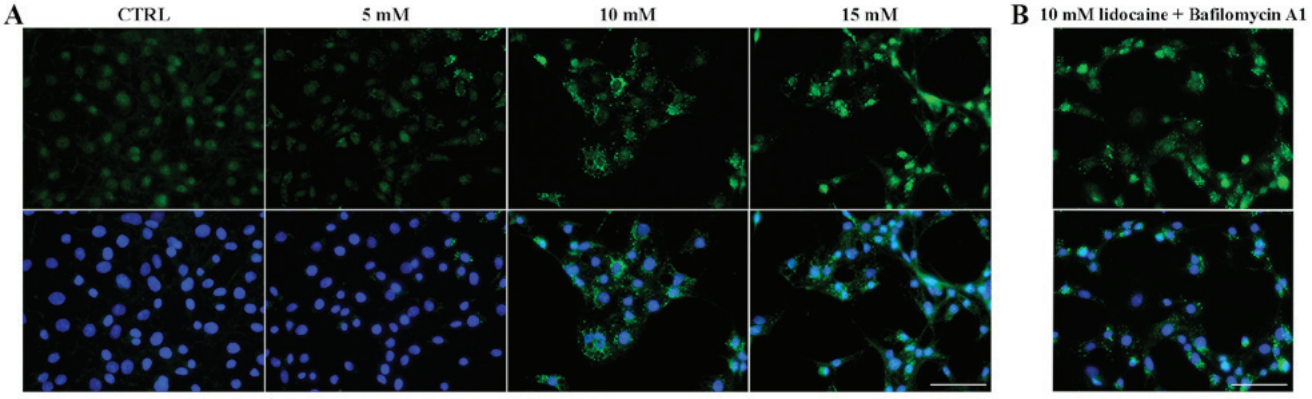

Figure 5. Detection of autophagy by LC3 accumulation. (A) Fluorescence staining of LC3-II (green) in CTRL cells, and cells treated with 5, 10 and 15 mM lidocaine; the cell nuclei were counterstained with DAPI (blue). Scale bar, 50 μm. (B) Negative control pretreated with Baf A1 (100 nM) and incubated with 10 mM lidocaine. Scale bar, 50 μm. Baf A1, bafilomycin A1; CTRL, control.

microtubule-organizing centers (MTOCs) (Fig. 8). Following treatment with higher doses lidocaine, a less dense network of microtubules formed compared with the control; however, the MTOCs were still visible (Fig. 8). Additionally, in shrunken cells a significantly higher fluorescence of tubulin was noticed (Fig. 8).

The last analyzed element of the cytoskeleton was vimentin. Analysis of actin and tubulin reorganization did not reveal vacuole-like structures, but after vimentin staining, autophagic vacuoles were detected. In control cells and cells treated with 5 mM lidocaine, extended intermediate filament networks in the cytoplasmic area and the accumulation of vimentin near the nucleolemma were observed. Following treatment with 10 and 15 mM lidocaine, vacuole-like structures surrounded by vimentin fibers were observed (Fig. 8).

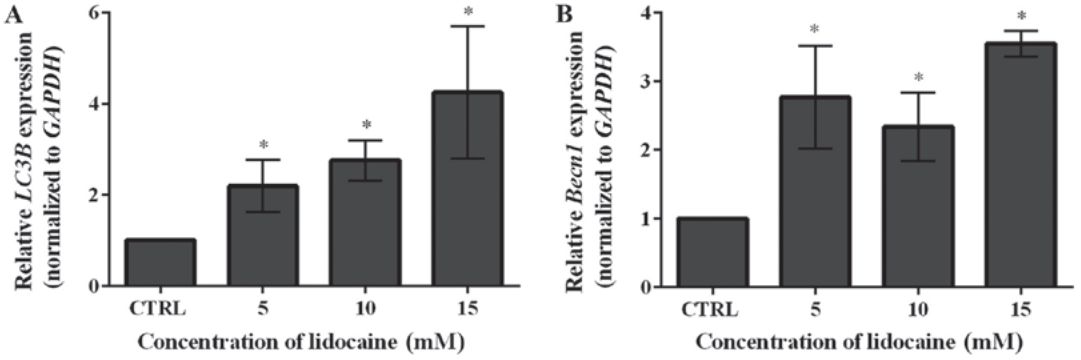

Figure 6. Reverse transcription-quantitative polymerase chain reaction. (A) LC3B and (B) Becn1 mRNA expression in CTRL cells, and cells treated with 5, 10 and 15 mM lidocaine. *P<0.05 vs. CTRL. Becn1, Beclin-1; CTRL, control; L3CB, microtubule-associated protein 1A/1B-light chain 3.

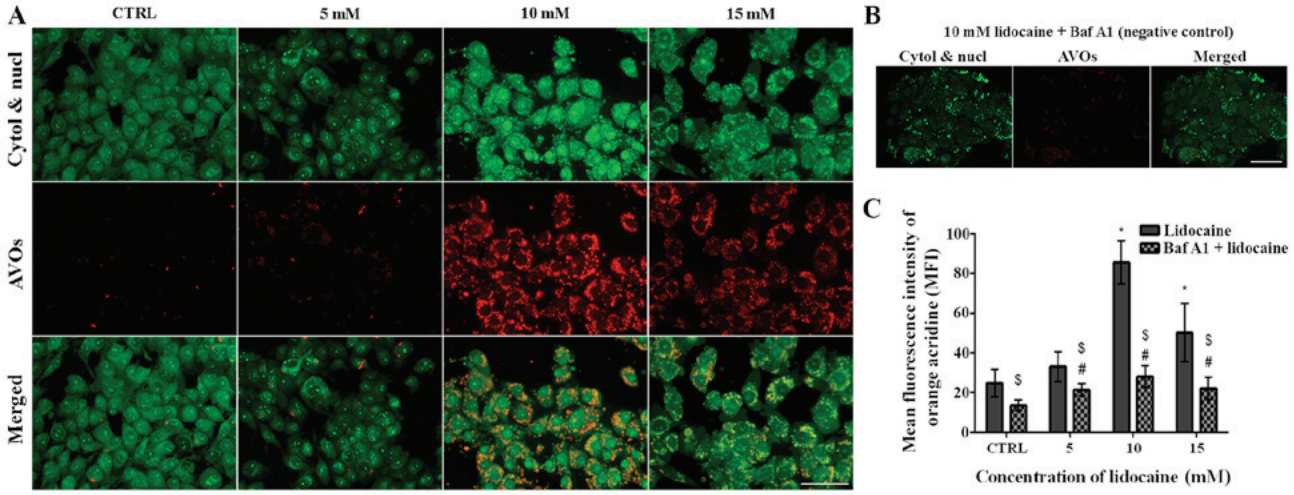

Figure 7. Detection of autophagy by acridine orange staining. (A) Fluorescence staining of AVOs (red fluorescence), as well as the cytoplasm and nucleus (green fluorescence) in control cells, and cells treated with 5, 10 and 15 mM lidocaine. Scale bar, 50 μm. (B) Negative control pretreated with Baf A1 (100 nM) and incubated with 10 mM lidocaine. Scale bar, 50 μm. (C) MFI of AO was determined using flow cytometer. *P<0.05 lidocaine doses vs. CTRL; #P<0.05 lidocaine doses + Baf A1 vs. CTRL + Baf A1. $P<0.05 cells pretreated with Baf A1 and then treated with lidocaine vs. cells treated just with lidocaine. AO, acridine orange, AVOs, acidic vesicular organelles; Baf A1, bafilomycin A1; CTRL, control; cytol, cytoplasm; MFI, mean fluorescence intensity; nucl, nucleus.

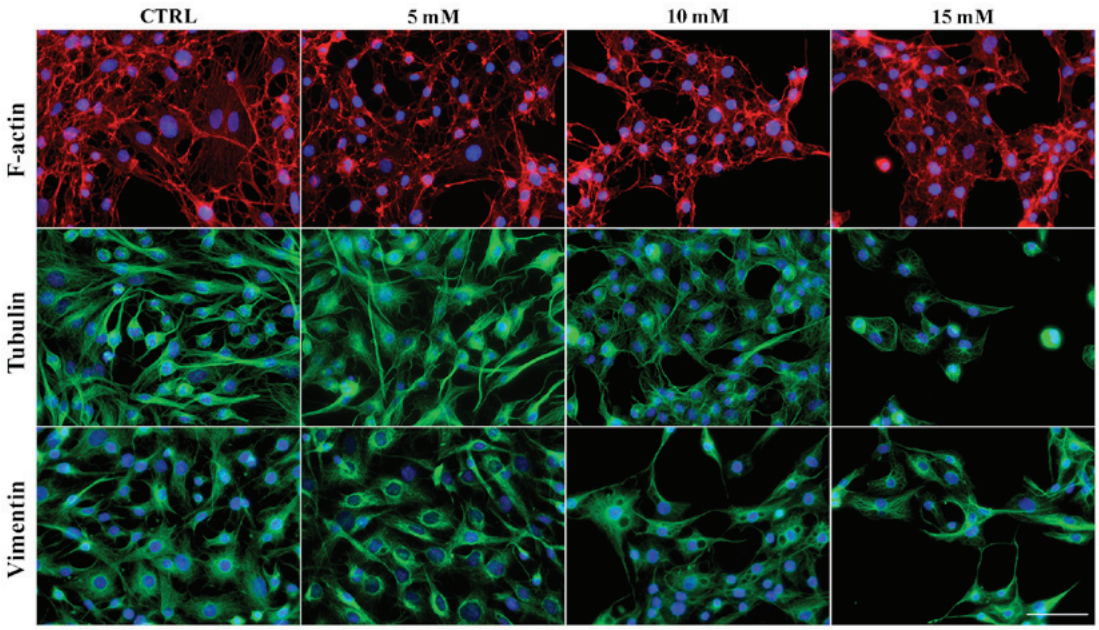

Figure 8. Fluorescence staining of the main cytoskeletal proteins. Fluorescence analysis of F-actin organization (red); tubulin (green) and vimentin (green) in the CTRL, and cells treated with 5, 10 and 15 mM lidocaine. Cell nuclei were counterstained with DAPI (blue). Scale bar, 50 μm.

Discussion

In the present study, the effects of lidocaine on the rat glioma C6 cell line were investigated. Malignant gliomas are primary brain tumors characterized by rapid and invasive growth (35). The standard treatment is based on radical brain tumor surgery, maximally safe radiation and concomitant chemotherapy (36-38). Despite the efforts of scientists and physicians to improve the effectiveness of treatment, further developments are required. Local anesthetics were reported as agents with the potential to notably inhibit tumor growth (17). One of them is lidocaine, which can be administered to local or regional tissue, and inhibits nerve conduction. Several studies have demonstrated lidocaine to suppress cell proliferation (28,39,40). Jurj *et al* (28) reported the antiproliferative effect of a clinical concentration of lidocaine on human hepatocarcinoma cells (HepG2). Other scientists revealed the antiproliferative, apoptotic and cytotoxic effect of this agent on various types of cancer cells. Sakaguchi *et al* (39) suggested that the inhibition of epidermal growth factor receptor activity by lidocaine is one way to decrease the proliferation of human tongue cancer cells (39). In addition, lidocaine enhances the therapeutic effect of drugs, including mitomycin C, pirarubicin and Su Fu'ning lotion in BIU-87 bladder cancer cells (40). Additionally, the combination of lidocaine with mitomycin C in mice with orthotopic bladder cancer resulted in prolonged survival and reduced tumor size (40). The antitumor effect of lidocaine on human breast cancer, hepatocellular carcinoma cells, non-small cell lung cancer cells and thyroid cancer cells was also observed (41-44). Furthermore, lidocaine was reported to suppress glioma cell proliferation (16,17). In the present study, a significant decrease in cell viability after incubation with 10, 15 and 30 mM lidocaine was observed compared with the control. Similar results of Leng *et al* (17) revealed the inhibition of proliferation of glioma cells (C6 rat glioma cell line and A172 human glioblastoma cell line) and indicated that lidocaine mediated this effect by decreasing the expression of TRPM7 channels.

Decreases in cell proliferation following treatment with cytostatic drugs or other agents are usually associated with the induction of cell death. Apoptosis is the most desirable type of cell death during cancer therapy. Lu *et al* (45) proposed that lidocaine induces alterations in intracellular calcium ion concentration and mitochondrial membrane potential in dose-dependent manners in U87-MG glioma cells by activating the overexpression of *TRPV1* to induce intrinsic apoptosis via the mitochondrial pathway (46). Cell death via the mitochondrial pathway induced by lidocaine is not restricted to glioma cells only, but is also activated in human hepatocellular carcinoma (HepG2), Jurkat T-lymphoma and human thyroid carcinoma (8505C) cells (16,44,47). Additionally, local anesthetic agents induce apoptosis via mitogen-activated protein kinase (13,44). Furthermore, numerous studies have reported that low doses of lidocaine induce the mitochondrial pathway of apoptosis (47-49). Li and Han (48) proposed that lidocaine in human neuroblastoma SH-SY5Y cells promoted endoplasmic reticulum stress-mediated apoptosis. In the present study, the apoptosis of C6 cells was noted, but the predominant type of cell death was necrosis. A similar effect was observed by Kamiya *et al* (50), in which lidocaine induced apoptosis at low concentrations and necrosis at much higher concentrations (>15 mM) in human histiocytic lymphoma cells. In human SHEP neuroblastoma cells, a high concentration of lidocaine (10 mM) promoted the transition from apoptosis to caspase-independent necrosis (47). Despite the induction of apoptosis and necrosis, the small vacuoles that were visible under the inverted microscope attracted our attention in the present study. Following hematoxylin staining of cells treated with 10 and 15 mM lidocaine, small enclosed compartments were observed. The present study proposed that these may have been autophagic vacuoles, and so were analyzed at the ultrastructural level. Using TEM, few of these structures contained amorphous materials and possibly the organelles at the various stages of degeneration. In cells of the other treatment groups, the vacuoles were empty and large. Additionally, what was not visible under the light microscope following treatment with the lowest dose of lidocaine, few, small vacuoles were observed. Similar findings at the ultrastructural were presented by Martinet *et al* (51), who described the protocol for studying autophagic vacuoles by TEM. On the basis of this data, it was assumed that lidocaine induced autophagy. Although the potential disadvantages of TEM methods make it impossible to limit research to only one method; the application of immunocytochemistry or immunohistochemistry, and molecular approaches for the unambiguous detection of autophagy are recommended.

Autophagy is a highly dynamic and regulated process, which is often accompanied by G0/G1 arrest; however, this is not required for the induction of autophagy (52). In the present study, significant alterations in the cell cycle distribution were reported in response to 5 and 10 mM lidocaine. The results are consistent with those of Xing *et al* (16), in which 5 mM lidocaine induced cell cycle arrest in G0/G1 in HepG2 cells, even if the main process of cell death was apoptosis. Additionally, autophagy is a very specific process, and can protect cancer cells to sustain their growth and survival in unfavorable conditions, such as the presence of cytostatic drugs; however, autophagy may be an alternative form of cell death (53). Therefore, autophagy may be exploited for cell survival under nutrient-restricted conditions, hypoxia or the cytotoxic effect of drugs; however, autophagic type II cell death may be therapeutically valuable and mediates the cytotoxic effects of anticancer drugs leading to tumor cell death (53,54). The autophagic process is associated with the formation and clearance of autophagosomes (55,56). The formation of these structures is directly associated with the cytosolic form of LC3 (LC3-I), which is conjugated to phosphatidylethanolamine and converted into LC3-phosphatidylethanolamine conjugate (LC3-II) (30,57). LC3-II is located in autophagosomal membranes; following the fusion of autophagosomes and lysosomes, the autophagosomal elements, such as LC3-II are hydrolyzed (30). Thus, LC3 protein and the formation of LC3-II are the main indicators of autophagy (30,51). In the present study, lidocaine treatment led to increased transcript levels of *LC3B*, which were the highest in glioma cells following treatment with 15 mM lidocaine. Similar results were obtained using fluorescence methods, which confirmed the findings of RT-qPCR analysis. The formation of autophagic vacuoles in the present study was increased by lidocaine, and the highest degree of LC3-II punctate staining was observed following treatment with 10 and 15 mM lidocaine. Xiong *et al* (58), described the effects of local anesthetic i.a. lidocaine on human neuroblastoma SH-SY5Y cells, and indicated increases in the

levels of LC3-II and the formation of autolysosomes using a dual fluorescence-based LC3 punctuation assay following the incubation of neuronal cells with lidocaine. Apart from LC3, autophagy is regulated by a series of regulators, such as Beclin-1, an essential initiator of autophagy (59,60). Beclin-1 serves a key role in the recruitment of autophagic proteins to the pre-autophagosomal structure, but also in the formation of the core complex, comprising Beclin-1, vacuolar protein sorting (Vps)34 and Vps15 (59). Of note, Beclin-1 is a factor which determines whether the cells undergo autophagy or apoptosis. This function is associated with interactions with anti-apoptotic proteins B-cell lymphoma-2 (Bcl-2) or Bcl-xL via its BH3 domain (59,61). This complex inhibits the assembly of the pre-autophagosomal structure, thereby suppressing autophagy (62). In autophagic cells, the levels of Beclin-1 are increased and those of Bcl-2 are decreased. In the present study, it was observed that lidocaine upregulated the mRNA expression of *Becn1*. The importance of increased Beclin-1 levels during autophagy was confirmed by Xiong *et al* (58). Autophagy inhibition was achieved by the transfection of cells with *Becn1* small interfering (si)RNA; knockdown in SH-SY5Y cells decreased LC3-II content, thereby suppressing cell viability (58). Reduction of Beclin-1 by siRNA resulted in defective autophagy and decreased the number of AVOs in human glioblastoma U87 and esophageal squamous cell carcinoma EC9706 cells (63,64).

The cytoskeleton is a very dynamic structure comprising microtubules, microfilaments and intermediate filaments. It is known that their organization and alterations are closely associated with the cell state (65,66). This organelle is involved in numerous cellular processes, including mitosis, proliferation, migration and cell death (67,68). In addition, the cytoskeleton is also involved in the autophagic process (69). The formation of actin branches by its reorganization is key for the biogenesis of autophagosomes. Actomyosin-based transport is used to feed the growing phagophore; finally, mature autophagosomes undergo intracellular transport and fusion with lysosomes and endosomes, with the involvement of actin, tubulin and signaling proteins (70).

Previously, the involvement of actin in autophagy was first observed by Aplin *et al* (71); F-actin depolymerizing drugs (cytochalasin D and latrunculin B) were reported to inhibit autophagosome formation and autophagy (71). At present, numerous studies have demonstrated that actin is involved in the autophagic process; however, as well as actin assembly and reorganization, actin may serve as a marker of autophagy (72,73). Numerous scientific reports proposed the association between the Arp 2/3 complex and actin polymerization during autophagy (74-77). It has been reported that the Arp 2/3 complex is capable of forming branched actin networks, which are important for all types of membrane remodeling activities in cells, as wells as autophagy (76,77). The present study proposed that actin filaments are important in the first steps of autophagy due to its colocalization with early omegasomes This suggests a role of actin in the initial steps of autophagosome formation. Following the induction of autophagy, actin networks bind the Arp 2/3 complex and polymerize inside the phagophore. This process is responsible for generating the shape (membrane curvature) of the autophagosomes and the fusion with lysosomes to form the autolysosomes. In mature autophagosomes, actin comet tails are formed (74,78). Additionally, the fusion of autophagosomes with lysosomes depends on the stability of actin filament branches, which is regulated by the well-known stabilizer of actin comprising the Arp 2/3 complex (71,78). The binding of the Arp 2/3 complex with cortactin and the depletion of cortactin results in the loss of the F-actin network, which inhibits autophagosome-lysosome fusion (79-81). In the present study, the reorganization of actin filaments was also observed.

Cells incubated with 10 mM lidocaine exhibited diffuse networks of F-actin with short actin fibers and/or small, punctate accumulations within the cytoplasm, and fibers of actin in the cortical region in the present study. This unstable form of actin may be associated with the continuous changes and dynamics of the autophagy process. The short fibers that are formed in autophagic cells are the components of the branched actin network.

Microtubules also undergo reorganization. Our study presents the importance of microtubule organization and microtubule-based motors in the autophagic process. Following the treatment of glioma cells with lidocaine, microtubules formed less dense networks compared with the control; MTOCs were still visible. This reorganization of the microtubule network may be associated with the stimulation of autophagosome formation. Additionally, the network of microtubules creates the pathway along which pre-autophagosomal structures and autophagosomes are transported (71). Destabilization of this cytoskeleton element delays the arrival of autophagosomes near lysosomes and thus, inhibits their fusion (69,82,83). Clearly visible MTOCs following treatment with lidocaine were noted in the present study. Jahreiss *et al* (83) reported that in rat kidney cells, lysosomes are localized at the perinuclear region about MTOCs, whereas autophagosomes form at the cortical region of the cells; thus autophagosomes translocate to the lysosomes in a microtubule-dependent manner (83). Similar results were obtained in cervical cancer cells, in which the MTOC-directed movement of these structures was associated with the microtubule network (84).

Intermediate filaments are also involved in the autophagic process. In the study presented by Ruangjaroon *et al* (85), in SH-SY5Y cells following treatment with 50 μM fipronil, vimentin formed a ring-like structure surrounding vacuoles. Identical localization of this protein was observed in the present study, which suggests that intermediate filaments serve an important role in the formation of autophagic vacuoles. In addition, vimentin can inhibit autophagy via a protein kinase B-dependent mechanism forming a complex with 14-3-3 protein and Beclin-1 (86).

However, confirmation regarding the nature of the autophagy observed is required as the activation of this process may be beneficial or harmful to cells (58). The pro-survival or pro-death mechanism of this process requires further investigation as to whether the increased rate of autophagy is due to the cellular response or resistance to treatment (87). To inhibit autophagy and obtain a negative control, the glioma cells were pretreated with Baf A1. Fluorescence analysis (AO and LC3II staining) revealed that lidocaine induced the autophagic process. Additionally, an MTT assay indicated that the incubation of cells with Baf A1 prior to lidocaine treatment (10 and

15 mM) significantly decreased the cell viability compared with in cells treated only with lidocaine. Furthermore, the addition of Baf A1 increased the number of apoptotic cells in response to higher doses of lidocaine. This suggests that lidocaine-induced autophagy may serve a protective role. Similar results have been reported by Xiong *et al* in which the protective mechanism of autophagy was suggested to be directed against neurotoxity of local anesthetics in human neuroblastoma cell line (58). Autophagy was inhibited via downregulation of Beclin-1; however, the same results were obtained via altering the expression of other proteins, which may be directly or indirectly involved in the process of autophagy (58,88,89). In addition, critical autophagy regulators are also cytoskeletal proteins involved in all stages of the process, and their stabilization or destabilization may affect the course of autophagy (71). There are numerous examples in which prosurvival autophagy occurs in response to chemotherapy. For instance, this process protects human breast cancer MCF-7 cells from epirubicin-induced apoptosis, and esophageal squamous carcinoma cells and colorectal cancer against the effects of 5-FU (90-92). In addition, several drugs indirectly associated with i.a. anesthetics may induce autophagy. The results of the present study may improve understanding of the effects of this process in different cancer cells, which may contribute to developments of novel therapeutic strategies for treatment of patients with glioma.

Acknowledgements

Not applicable.

Funding

The present study was co-supported via research tasks within the framework of statutory activities no. 294 (Nicolaus Copernicus University in Toruń, Faculty of Medicine, Collegium Medicum in Bydgoszcz).

Availability of data and materials

The data and materials described in manuscript are available upon request.

Authors' contributions

MI made substantial contributions to the design of the resent study and supervised its quality. MI, WZ, MHW and AKW wrote this paper and performed the experiments. MG and DG made substantial contributions in collecting all the data and analyzed the data in the study. MI, WZ and MHW critically revised the manuscript for important intellectual content. All authors have read and approved the final manuscript.

Ethics approval and consent to participate

Not applicable.

Patient consent for publication

Not applicable.

Competing interests

The authors declare that they have no competing interests.

References

1. Goodenberger ML and Jenkins RB: Genetics of adult glioma. Cancer Genet 205: 613-621, 2012.
2. Ohgaki H and Kleihues P: Population-based studies on incidence, survival rates, and genetic alterations in astrocytic and oligodendroglial gliomas. J Neuropathol Exp Neurol 64: 479-489, 2005.
3. Bleeker FE, Molenaar RJ and Leenstra S: Recent advances in the molecular understanding of glioblastoma. J Neurooncol 108: 11-27, 2012.
4. Burdett S and Stewart L; Glioma Meta-Analysis Trialists Group: Chemotherapy for high-grade glioma. Neuroepidemiology 22: 366, 2003.
5. Neeman E and Ben-Eliyahu S: Surgery and stress promote cancer metastasis: New outlooks on perioperative mediating mechanisms and immune involvement. Brain Behav Immun 30 (Suppl): S32-S40, 2013.
6. Gottschalk A, Sharma S, Ford J, Durieux ME and Tiouririne M: Review article: The role of the perioperative period in recurrence after cancer surgery. Anesth Analg 110: 1636-1643, 2010.
7. Roger S, Rollin J, Barascu A, Besson P, Raynal PI, Iochmann S, Lei M, Bougnoux P, Gruel Y and Le Guennec JY: Voltage-gated sodium channels potentiate the invasive capacities of human non-small-cell lung cancer cell lines. Int J Biochem Cell Biol 39: 774-786, 2007.
8. Gao R, Shen Y, Cai J, Lei M and Wang Z: Expression of voltage-gated sodium channel alpha subunit in human ovarian cancer. Oncol Rep 23: 1293-1299, 2010.
9. Diss JK, Archer SN, Hirano J, Fraser SP and Djamgoz MB: Expression profiles of voltage-gated Na(+) channel alpha-subunit genes in rat and human prostate cancer cell lines. Prostate 48: 165-178, 2001.
10. Yang M, Kozminski DJ, Wold LA, Modak R, Calhoun JD, Isom LL and Brackenbury WJ: Therapeutic potential for phenytoin: Targeting Na(v)1.5 sodium channels to reduce migration and invasion in metastatic breast cancer. Breast Cancer Res Treat 134: 603-615, 2012.
11. Grimes JA, Fraser SP, Stephens GJ, Downing JEG, Laniado ME, Foster CS, Abel PD and Djamgoz MBA: Differential expression of voltage-activated Na^+ currents in two prostatic tumour cell lines: Contribution to invasiveness in vitro. FEBS Lett 369: 290-294, 1995.
12. Laniado ME, Lalani EN, Fraser SP, Grimes JA, Bhangal G, Djamgoz MB and Abel PD: Expression and functional analysis of voltage-activated Na^+ channels in human prostate cancer cell lines and their contribution to invasion in vitro. Am J Pathol 150: 1213-1221, 1997.
13. Wang HW, Wang LY, Jiang L, Tian SM, Zhong TD and Fang XM: Amide-linked local anesthetics induce apoptosis in human non-small cell lung cancer. J Thorac Dis 8: 2748-2757, 2016.
14. Piegeler T, Votta-Velis EG, Liu G, Place AT, Schwartz DE, Beck-Schimmer B, Minshall RD and Borgeat A: Antimetastatic potential of amide-linked local anesthetics: Inhibition of lung adenocarcinoma cell migration and inflammatory Src signaling independent of sodium channel blockade. Anesthesiology 117: 548-559, 2012.
15. Lirk P, Berger R, Hollmann MW and Fiegl H: Lidocaine time- and dose-dependently demethylates deoxyribonucleic acid in breast cancer cell lines in vitro. Br J Anaesth 110: 165, 2013.
16. Xing W, Chen DT, Pan JH, Chen YH, Yan Y, Li Q, Xue RF, Yuan YF and Zeng WA: Lidocaine induces apoptosis and suppresses tumor growth in human hepatocellular carcinoma cells in vitro and in a xenograft model in vivo. Anesthesiology 126: 868-881, 2017.
17. Leng T, Lin S, Xiong Z and Lin J: Lidocaine suppresses glioma cell proliferation by inhibiting TRPM7 channels. Int J Physiol Pathophysiol Pharmacol 9: 8-15, 2017.
18. Johnson ME, Saenz JA, DaSilva AD, Uhl CB and Gores GJ: Effect of local anesthetic on neuronal cytoplasmic calcium and plasma membrane lysis (necrosis) in a cell culture model. Anesthesiology 97: 1466-1476, 2002.
19. Johnson ME, Uhl CB, Spittler KH, Wang H and Gores GJ: Mitochondrial injury and caspase activation by the local anesthetic lidocaine. Anesthesiology 101: 1184-1194, 2004.

20. Lirk P, Haller I, Hausott B, Ingorokva S, Deibl M, Gerner P and Klimaschewski L: The neurotoxic effects of amitriptyline are mediated by apoptosis and are effectively blocked by inhibition of caspase activity. Anesth Analg 102: 1728-1733, 2006.
21. Glick D, Barth S and Macleod KF: Autophagy: Cellular and molecular mechanisms. J Pathol 221: 3-12, 2010.
22. Qu X, Yu J, Bhagat G, Furuya N, Hibshoosh H, Troxel A, Rosen J, Eskelinen EL, Mizushima N, Ohsumi Y, *et al*: Promotion of tumorigenesis by heterozygous disruption of the beclin 1 autophagy gene. J Clin Invest 112: 1809-1820, 2003.
23. Yue Z, Jin S, Yang C, Levine AJ and Heintz N: Beclin 1, an autophagy gene essential for early embryonic development, is a haploinsufficient tumor suppressor. Proc Natl Acad Sci USA 100: 15077-15082, 2003.
24. Mariño G, Salvador-Montoliu N, Fueyo A, Knecht E, Mizushima N and López-Otín C: Tissue-specific autophagy alterations and increased tumorigenesis in mice deficient in Atg4C/autophagin-3. J Biol Chem 282: 18573-18583, 2007.
25. Ekiz HA, Can G and Baran Y: Role of autophagy in the progression and suppression of leukemias. Crit Rev Oncol Hematol 81: 275-285, 2012.
26. Izdebska M, Klimaszewska-Wiśniewska A, Hałas M, Gagat M and Grzanka A: Green tea extract induces protective autophagy in A549 non-small lung cancer cell line. Postepy Hig Med Dosw (Online) 69: 1478-1484, 2015.
27. Livak KJ and Schmittgen TD: Analysis of relative gene expression data using real-time quantitative PCR and the 2(-ΔΔC(T)) method. Methods 25: 402-408, 2001.
28. Jurj A, Tomuleasa C, Tat TT, Berindan-Neagoe I, Vesa SV and Ionescu DC: Antiproliferative and apoptotic effects of lidocaine on human hepatocarcinoma cells. A preliminary study. J Gastrointestin Liver Dis 26: 45-50, 2017.
29. Klionsky DJ, Elazar Z, Seglen PO and Rubinsztein DC: Does bafilomycin A1 block the fusion of autophagosomes with lysosomes? Autophagy 4: 849-850, 2008.
30. Tanida I, Ueno T and Kominami E: LC3 and autophagy. Methods Mol Biol 445: 77-88, 2008.
31. Lee YK and Lee JA: Role of the mammalian ATG8/LC3 family in autophagy: Differential and compensatory roles in the spatiotemporal regulation of autophagy. BMB Rep 49: 424-430, 2016.
32. Paglin S, Hollister T, Delohery T, Hackett N, McMahill M, Sphicas E, Domingo D and Yahalom J: A novel response of cancer cells to radiation involves autophagy and formation of acidic vesicles. Cancer Res 61: 439-444, 2001.
33. Izdebska M, Zielińska W, Grzanka D and Gagat M: The role of actin dynamics and actin-binding proteins expression in epithelial-to-mesenchymal transition and its association with cancer progression and evaluation of possible therapeutic targets. BioMed Res Int 2018: 4578373, 2018.
34. Grzanka D, Gagat M and Izdebska M: Involvement of the SATB1/F-actin complex in chromatin reorganization during active cell death. Int J Mol Med 33: 1441-1450, 2014.
35. Sampetrean O and Saya H: Modeling phenotypes of malignant gliomas. Cancer Sci 109: 6-14, 2018.
36. Nakada M, Nakada S, Demuth T, Tran NL, Hoelzinger DB and Berens ME: Molecular targets of glioma invasion. Cell Mol Life Sci 64: 458-478, 2007.
37. Li G, Qin Z, Chen Z, Xie L, Wang R and Zhao H: Tumor microenvironment in treatment of glioma. Open Med (Wars) 12: 247-251, 2017.
38. Mostovenko E, Végvári Á, Rezeli M, Lichti CF, Fenyö D, Wang Q, Lang FF, Sulman EP, Sahlin KB, Marko-Varga G, *et al*: Large scale identification of variant proteins in glioma stem cells. ACS Chem Neurosci 9: 73-79, 2018.
39. Sakaguchi M, Kuroda Y and Hirose M: The antiproliferative effect of lidocaine on human tongue cancer cells with inhibition of the activity of epidermal growth factor receptor. Anesth Analg 102: 1103-1107, 2006.
40. Yang X, Zhao L, Li M, Yan L, Zhang S, Mi Z, Ren L and Xu J: Lidocaine enhances the effects of chemotherapeutic drugs against bladder cancer. Sci Rep 8: 598, 2018.
41. Chamaraux-Tran TN, Mathelin C, Aprahamian M, Joshi GP, Tomasetto C, Diemunsch P and Akladios C: Antitumor effects of lidocaine on human breast cancer cells: An in vitro and in vivo experimental trial. Anticancer Res 38: 95-105, 2018.
42. Le Gac G, Angenard G, Clément B, Laviolle B, Coulouarn C and Beloeil H: Local anesthetics inhibit the growth of human hepatocellular carcinoma cells. Anesth Analg 125: 1600-1609, 2017.
43. Zhang L, Hu R, Cheng Y, Wu X, Xi S, Sun Y and Jiang H: Lidocaine inhibits the proliferation of lung cancer by regulating the expression of GOLT1A. Cell Prolif 50: 50, 2017.
44. Chang YC, Hsu YC, Liu CL, Huang SY, Hu MC and Cheng SP: Local anesthetics induce apoptosis in human thyroid cancer cells through the mitogen-activated protein kinase pathway. PLoS One 9: e89563, 2014.
45. Lu J, Ju YT, Li C, Hua FZ, Xu GH and Hu YH: Effect of TRPV1 combined with lidocaine on cell state and apoptosis of U87-MG glioma cell lines. Asian Pac J Trop Med 9: 288-292, 2016.
46. Martinou JC and Youle RJ: Mitochondria in apoptosis: Bcl-2 family members and mitochondrial dynamics. Dev Cell 21: 92-101, 2011.
47. Werdehausen R, Braun S, Essmann F, Schulze-Osthoff K, Walczak H, Lipfert P and Stevens MF: Lidocaine induces apoptosis via the mitochondrial pathway independently of death receptor signaling. Anesthesiology 107: 136-143, 2007.
48. Li K and Han X: Endoplasmic reticulum stress is involved in the lidocaine-induced apoptosis in SH-SY5Y neuroblastoma cells. J Mol Neurosci 56: 122-130, 2015.
49. Kawasaki C, Kawasaki T, Ogata M, Sata T and Chaudry IH: Lidocaine enhances apoptosis and suppresses mitochondrial functions of human neutrophil in vitro. J Trauma 68: 401-408, 2010.
50. Kamiya Y, Ohta K and Kaneko Y: Lidocaine-induced apoptosis and necrosis in U937 cells depending on its dosage. Biomed Res 26: 231-239, 2005.
51. Martinet W, Timmermans JP and De Meyer GRY: Methods to assess autophagy in situ - transmission electron microscopy versus immunohistochemistry. Methods Enzymol 543: 89-114, 2014.
52. Valentin M and Yang E: Autophagy is activated, but is not required for the G0 function of BCL-2 or BCL-xL. Cell Cycle 7: 2762-2768, 2008.
53. Reyjal J, Cormier K and Turcotte S: Autophagy and cell death to target cancer cells: Exploiting synthetic lethality as cancer therapies. Adv Exp Med Biol 772: 167-188, 2014.
54. Eskelinen EL: The dual role of autophagy in cancer. Curr Opin Pharmacol 11: 294-300, 2011.
55. Zhou J, Hu SE, Tan SH, Cao R, Chen Y, Xia D, Zhu X, Yang XF, Ong CN and Shen HM: Andrographolide sensitizes cisplatin-induced apoptosis via suppression of autophagosome-lysosome fusion in human cancer cells. Autophagy 8: 338-349, 2012.
56. Chen G, Ke Z, Xu M, Liao M, Wang X, Qi Y, Zhang T, Frank JA, Bower KA, Shi X, *et al*: Autophagy is a protective response to ethanol neurotoxicity. Autophagy 8: 1577-1589, 2012.
57. Yin Z, Pascual C and Klionsky DJ: Autophagy: Machinery and regulation. Microb Cell 3: 588-596, 2016.
58. Xiong J, Kong Q, Dai L, Ma H, Cao X, Liu L and Ding Z: Autophagy activated by tuberin/mTOR/p70S6K suppression is a protective mechanism against local anaesthetics neurotoxicity. J Cell Mol Med 21: 579-587, 2017.
59. Kang R, Zeh HJ, Lotze MT and Tang D: The Beclin 1 network regulates autophagy and apoptosis. Cell Death Differ 18: 571-580, 2011.
60. Wirawan E, Lippens S, Vanden Berghe T, Romagnoli A, Fimia GM, Piacentini M and Vandenabeele P: Beclin1: A role in membrane dynamics and beyond. Autophagy 8: 6-17, 6-17, 2012.
61. Decuypere JP, Parys JB and Bultynck G: Regulation of the autophagic Bcl-2/Beclin 1 interaction. Cells 1: 284-312, 2012
62. Marquez RT and Xu L: Bcl-2:Beclin 1 complex: multiple, mechanisms regulating autophagy/apoptosis toggle switch. Am J Cancer Res 2: 214-221, 2012.
63. Huang X, Qi Q, Hua X, Li X, Zhang W, Sun H, Li S, Wang X and Li B: Beclin 1, an autophagy-related gene, augments apoptosis in U87 glioblastoma cells. Oncol Rep 31: 1761-1767, 2014.
64. Du H, Che J, Shi M, Zhu L, Hang JB, Chen Z and Li H: Beclin 1 expression is associated with the occurrence and development of esophageal squamous cell carcinoma. Oncol Lett 14: 6823-6828, 2017.
65. Pawlak G and Helfman DM: Cytoskeletal changes in cell transformation and tumorigenesis. Curr Opin Genet Dev 11: 41-47, 2001.
66. Pegoraro AF, Janmey P and Weitz DA: Mechanical properties of the cytoskeleton and cells. Cold Spring Harb Perspect Biol 9: a022038, 2017.
67. Hall A: The cytoskeleton and cancer. Cancer Metastasis Rev 28: 5-14, 2009.
68. Pollard TD: The cytoskeleton, cellular motility and the reductionist agenda. Nature 422: 741-745, 2003.
69. Kast DJ and Dominguez R: The cytoskeleton-autophagy connection. Curr Biol 27: R318-R326, 2017.
70. Kruppa AJ, Kendrick-Jones J and Buss F: Myosins, actin and autophagy. Traffic 17: 878-890, 2016.

71. Aplin A, Jasionowski T, Tuttle DL, Lenk SE and Dunn WA Jr: Cytoskeletal elements are required for the formation and maturation of autophagic vacuoles. J Cell Physiol 152: 458-466, 1992.
72. Aguilera MO, Berón W and Colombo MI: The actin cytoskeleton participates in the early events of autophagosome formation upon starvation induced autophagy. Autophagy 8: 1590-1603, 2012.
73. Reggiori F, Monastyrska I, Shintani T and Klionsky DJ: The actin cytoskeleton is required for selective types of autophagy, but not nonspecific autophagy, in the yeast Saccharomyces cerevisiae. Mol Biol Cell 16: 5843-5856, 2005.
74. Monastyrska I, He C, Geng J, Hoppe AD, Li Z and Klionsky DJ: Arp2 links autophagic machinery with the actin cytoskeleton. Mol Biol Cell 19: 1962-1975, 2008.
75. Monastyrska I, Rieter E, Klionsky DJ and Reggiori F: Multiple roles of the cytoskeleton in autophagy. Biol Rev Camb Philos Soc 84: 431-448, 2009.
76. Kast DJ, Zajac AL, Holzbaur EL, Ostap EM and Dominguez R: WHAMM directs the Arp2/3 complex to the ER for autophagosome biogenesis through an actin comet tail mechanism. Curr Biol 25: 1791-1797, 2015.
77. Mi N, Chen Y, Wang S, Chen M, Zhao M, Yang G, Ma M, Su Q, Luo S, Shi J, *et al*: CapZ regulates autophagosomal membrane shaping by promoting actin assembly inside the isolation membrane. Nat Cell Biol 17: 1112-1123, 2015.
78. Coutts AS and La Thangue NB: Regulation of actin nucleation and autophagosome formation. Cell Mol Life Sci 73: 3249-3263, 2016.
79. Fehrenbacher K, Huckaba T, Yang HC, Boldogh I and Pon L: Actin comet tails, endosomes and endosymbionts. J Exp Biol 206: 1977-1984, 2003.
80. Taunton J, Rowning BA, Coughlin ML, Wu M, Moon RT, Mitchison TJ and Larabell CA: Actin-dependent propulsion of endosomes and lysosomes by recruitment of N-WASP. J Cell Biol 148: 519-530, 2000.
81. Lee JY, Koga H, Kawaguchi Y, Tang W, Wong E, Gao YS, Pandey UB, Kaushik S, Tresse E, Lu J, *et al*: HDAC6 controls autophagosome maturation essential for ubiquitin-selective quality-control autophagy. EMBO J 29: 969-980, 2010.
82. Mackeh R, Perdiz D, Lorin S, Codogno P and Poüs C: Autophagy and microtubules - new story, old players. J Cell Sci 126: 1071-1080, 2013.
83. Jahreiss L, Menzies FM and Rubinsztein DC: The itinerary of autophagosomes: From peripheral formation to kiss-and-run fusion with lysosomes. Traffic 9: 574-587, 2008.
84. Kimura S, Noda T and Yoshimori T: Dynein-dependent movement of autophagosomes mediates efficient encounters with lysosomes. Cell Struct Funct 33: 109-122, 2008.
85. Ruangjaroon T, Chokchaichamnankit D, Srisomsap C, Svasti J and Parichartanakul NM: Involvement of vimentin in neurite outgrowth damage induced by fipronil in SH-SY5Y cells. Biochem Biophys Res Commun 486: 652-658, 2017.
86. Wang RC, Wei Y, An Z, Zou Z, Xiao G, Bhagat G, White M, Reichelt J and Levine B: Akt-mediated regulation of autophagy and tumorigenesis through Beclin 1 phosphorylation. Science 338: 956-959, 2012.
87. Sui X, Chen R, Wang Z, Huang Z, Kong N, Zhang M, Han W, Lou F, Yang J, Zhang Q, *et al*: Autophagy and chemotherapy resistance: A promising therapeutic target for cancer treatment. Cell Death Dis 4: e838, 2013.
88. Redmann M, Benavides GA, Berryhill TF, Wani WY, Ouyang X, Johnson MS, Ravi S, Barnes S, Darley-Usmar VM and Zhang J: Inhibition of autophagy with bafilomycin and chloroquine decreases mitochondrial quality and bioenergetic function in primary neurons. Redox Biol 11: 73-81, 2017.
89. Yang YP, Hu LF, Zheng HF, Mao CJ, Hu WD, Xiong KP, Wang F and Liu CF: Application and interpretation of current autophagy inhibitors and activators. Acta Pharmacol Sin 34: 625-635, 2013.
90. Sun WL, Chen J, Wang YP and Zheng H: Autophagy protects breast cancer cells from epirubicin-induced apoptosis and facilitates epirubicin-resistance development. Autophagy 7: 1035-1044, 2011.
91. Liu D, Yang Y, Liu Q and Wang J: Inhibition of autophagy by 3-MA potentiates cisplatin-induced apoptosis in esophageal squamous cell carcinoma cells. Med Oncol 28: 105-111, 2011.
92. Li J, Hou N, Faried A, Tsutsumi S and Kuwano H: Inhibition of autophagy augments 5-fluorouracil chemotherapy in human colon cancer in vitro and in vivo model. Eur J Cancer 46: 1900-1909, 2010.